Reconstructing the Invasive History and Potential Distribution Prediction of *Amaranthus palmeri* in China

Xinyu Jiao [†], Mei Long [†], Jiayi Li, Qingyu Yang and Zhixiong Liu *

College of Horticulture and Gardening, Yangtze University, Jingzhou 434025, China;
2021720874@yangtzeu.edu.cn (X.J.); 2021720867@yangtzeu.edu.cn (M.L.); 2021710820@yangtzeu.edu.cn (J.L.);
2021710827@yangtzeu.edu.cn (Q.Y.)
* Correspondence: zxliu@yangtzeu.edu.cn
[†] These authors contributed equally to this work.

Abstract: Palmer Amaranth (*Amaranthus palmeri*, Amaranthaceae) is one of the most competitive, troublesome, and noxious weeds causing significant yield reductions in various crops. *A. palmeri* was also a herbicide-resistant weed causing a serious eco-environmental problem. Given that the process of invasion is dynamic, the *A. plamer* invasion may already be quite severe where invasive species management and surveys are chronically lacking. Predicting the potential habitat of *A. palmeri* can help to develop effective measures for early warning and long-term detection. However, the invasive history and distribution patterns of *A. palmeri* in China remain largely unknown. Here, the invasive history and distribution patterns of *A. palmeri* from 1985 to 2022 in China were reconstructed, and then the potential geographical distribution of *A. palmeri* was predicted under current and future climate scenarios (SSP1-2.6, SSP2-4.5, SSP5-8.5) using the optimal MaxEnt model (V 3.4.4) and ArcGIS 10.8.2. The mean AUC values of *A. palmeri* were 0.967. Under the current climate conditions, the suitable habitat areas for *A. palmeri* reached 1,067,000 km^2 in China and were mainly distributed in north and central China. Under the future scenarios, the highly suitable habitats were mainly distributed in Beijing, Tianjin, and Hebei. Under SSP2–4.5, the future suitable areas will reach the maximum and expand to 1,411,100 km^2 in the 2060s. The centroid distribution would northwestward extend under future climate scenarios. The human footprint index, mean temperature of the warmest quarter (Bio_10), April wind speed (Wind_4), temperature seasonality (standard deviation $\times$ 100) (bio_4), topsoil gravel content (T_gravel), and precipitation of warmest quarter (Bio_18) were key environmental variables affecting distribution and growth of *A. palmeri*. Climate change would increase the risk of *A. palmeri* expanding to high latitudes. Our results will help in developing effective strategies for the early warning, prevention, control, and management of *A. palmeri* in China.

Keywords: invasive alien plants; *Amaranthus palmeri*; optimize Maxent model; driving factors; climate change

1. Introduction

Biological invasions are becoming a common feature of ecosystems worldwide and are one of the main drivers of biodiversity changes in recent years [1]. Biological invasions are not only responsible for substantial biodiversity declines as well as huge economic losses to society and monetary expenditures associated with the management of these invasions, but also responsible for tremendous impacts globally on our socio-ecosystems [2,3]. Invasive species can alter the structure and functioning of ecosystems and impact ecosystem services and human health and well-being [4,5]. Moreover, invasive species could incur huge economic costs in many sectors, notably agriculture, forestry, fisheries, aquaculture, and nature conservation [4].

Palmer Amaranth (*Amaranthus palmeri*) is a dioecious species belonging to the family Amaranthaceae, and one of the most competitive troublesome and economically damaging

weeds due to its high genetic diversity, rapid growth rates, high seed production, and high vigour [6,7] Moreover, *A. palmeri* is one of the most noxious weeds causing significant yield reductions in various crops [8]. *A. palmeri* was also a herbicide-resistant weed and originated from the deserts of Southwestern United States and Mexico. In recent years, *A. palmeri* was reportedly introduced to South America, Asia, Europe, Argentina, Brazil, and other regions of the world [9]. Moreover, *A. palmeri* has been ranked as the worst weed in the United States cropping systems and has evolved resistance rapidly and repeatedly to the widely used herbicide (glyphosate), requiring the development of non-chemical methods to control this weed in agricultural and non-agricultural habitats [7,10,11]. Furthermore, *A. palmeri* can transfer herbicide-resistance genes to other closely related weeds through interspecific hybridization, posing the risk of forming the world's worst weeds [12,13]. This herbicide-resistant weed was first reported in Beijing in 1985 and has invaded multiple areas of China in recent decades [9,14]. However, the invasive dynamics and potential distribution patterns of *A. palmeri* in China remain largely unknown. So, it is critical to assess the invasive populations in China and develop more efficient management strategies to control new invasions as early as possible.

The invasion of exotic plants is thought to be a result of globalization, agriculture, and human activity [15,16]. In invasive exotic plant management, the prevention of a novel exotic plant reaching a new location is key to reducing unwanted invasions. Prior to species establishment, early detection followed by control and eradication is the most effective course of action in reducing spread [17]. Inferring invasion histories is a basic requirement to develop suitable management strategies for predicting their future dispersal and consequently developing strategies for prevention and eradication [18,19]. Moreover, it is also crucial to understand what extent invaders adapted to novel environments, along with the mechanisms of such adaptations [19].

Multiple abiotic and biotic factors need to be considered to reveal the patterns of the invasion process more precisely [20–22]. However, previous studies only examined the effects of climate and land cover on *A. palmeri* [23,24], so it is necessary to examine the effects of soil properties, human activities such as transportation construction, and trade activities [14]. Therefore, in this study, we reconstruct the invasive history and distribution patterns of *A. palmeri* from 1985 to 2022 in China by integrating historical records, preserving herbarium specimens, and conducting field research. Furthermore, we predict the potential geographical distribution of *A. palmeri* throughout China under current and future climate scenarios using the optimal MaxEnt model (V 3.4.4). In order to screen the key factors driving the distribution and spread of *A. palmeri*, the relationship between the environmental factors, such as climatic variables, topography, soil factors, and human activities (human land use, infrastructure development, population density, NOAA night light data, data layers obtained by normalizing roads and railways layers), and the distribution of *A. palmeri* were analyzed using optimize Maxent model (V 3.4.4) with Jackknife method in China. Our results provide a practical reference for the early warning, prevention, control, and management of *A. palmeri* in China.

2. Materials and Methods

The operational step-by-step methods are described herein (Figure 1): (1) collection and processing of *A. palmeri* distribution and environmental data (first step); (2) research on the spread dynamics and historical reconstruction of *A. palmeri* in China (second step); (3) optimization and evaluation of the Maxent model (V 3.4.4) utilizing the R programming language 3.6.3 and ENMtools 1.0 (third step); (4) result analysis, including the ranking classification of the suitable area for *A. palmeri* and its space evolution characteristics under current and different future climate change scenarios (fourth step).
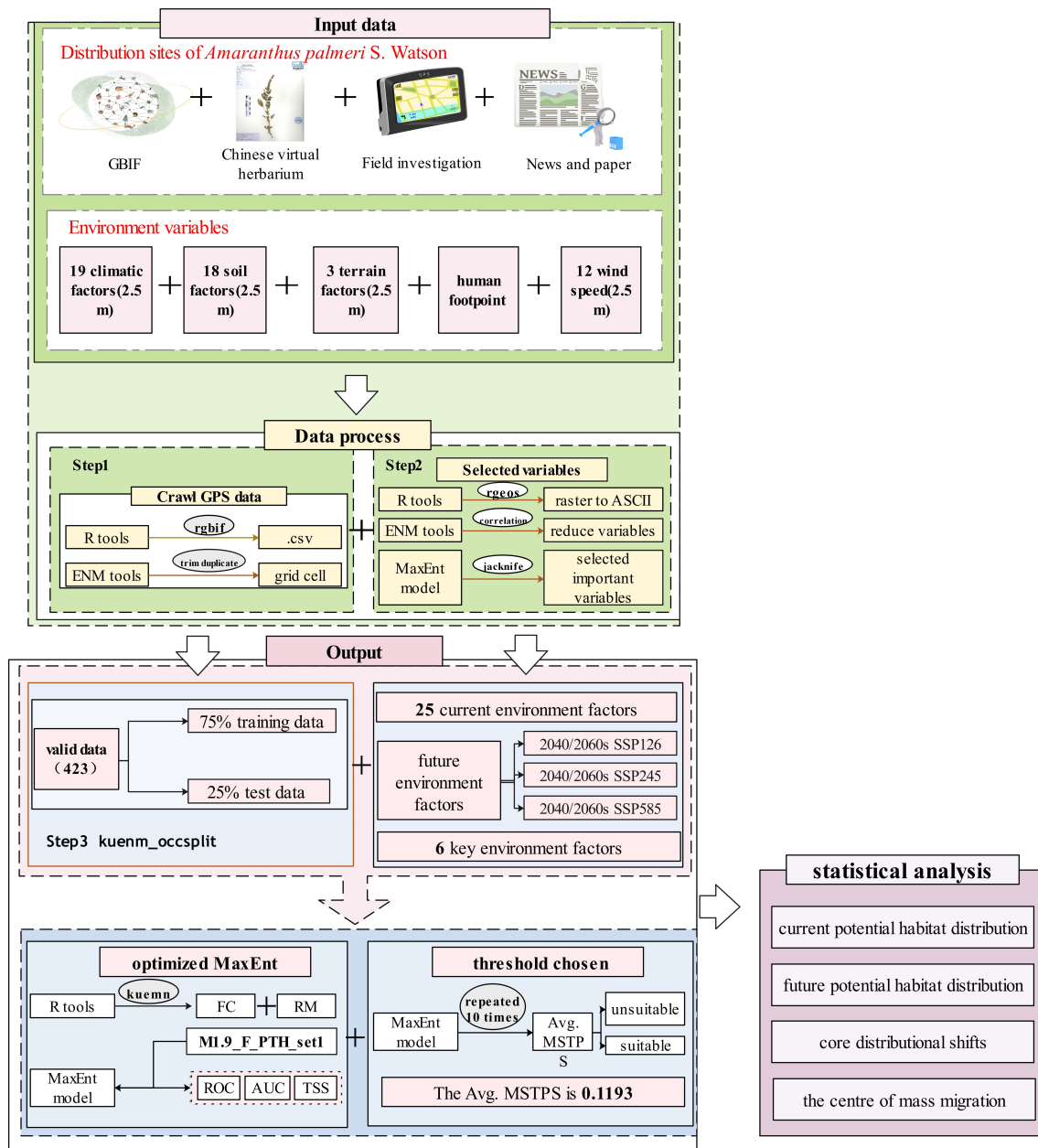
Figure 1. Technology Roadmap.

2.1. Data Process

(1)　Occurrence records

　　A. palmeri occurrence records were collected from the Global Biodiversity Information Facility (GBIF; https://www.gbif.org/, accessed on 12 April 2023), Chinese virtual herbarium (CHV; https://www.cvh.ac.cn/, accessed on 11 April 2023), Plant Photo Bank of China (PPBC; http://ppbc.iplant.cn/, accessed on 13 April 2023), and our survey data. Moreover, the Web of Science (WOS; https://www.webofscience.com/, accessed on 13 April 2023) database was searched by using the scientific names of the target species and China for collecting recorded all the species distribution sites reported in the literature. In addition, the China National Knowledge Infrastructure (CNKI; https://www.cnki.net/, accessed on 15 April 2023) database (the largest and most complete database for Chinese scientific studies) was searched by using both Chinese and scientific names of our target species as

keywords and referred to related reports news [14,25]. A total of 581 actual distribution sites of *A. palmeri* were collected.

The geographic distribution data of *A. palmeri* were further processed using ArcGIS 10.8.2 software as follows: first, the exact longitude and latitude of each collection site were obtained using bigemap software (30.0.0); secondly, whether the reported latitudes and longitudes matched the collection sites were checked one by one; and then, in order to mitigate the sampling bias of the data and avoid the spatial autocorrelation caused by duplicated coordinates and too close coordinates, the distribution sites data were screened using "trim duplicate" in the ENMtools (https://github.com/danlwarren/ENMTools, accessed on 23 April 2023) software 1.0 described by Yang et al. [26], and ensure that there is only one observation in each 2.5 × 2.5 km raster grid. 423 valid data of *A. palmeri* were obtained (Figure 2).
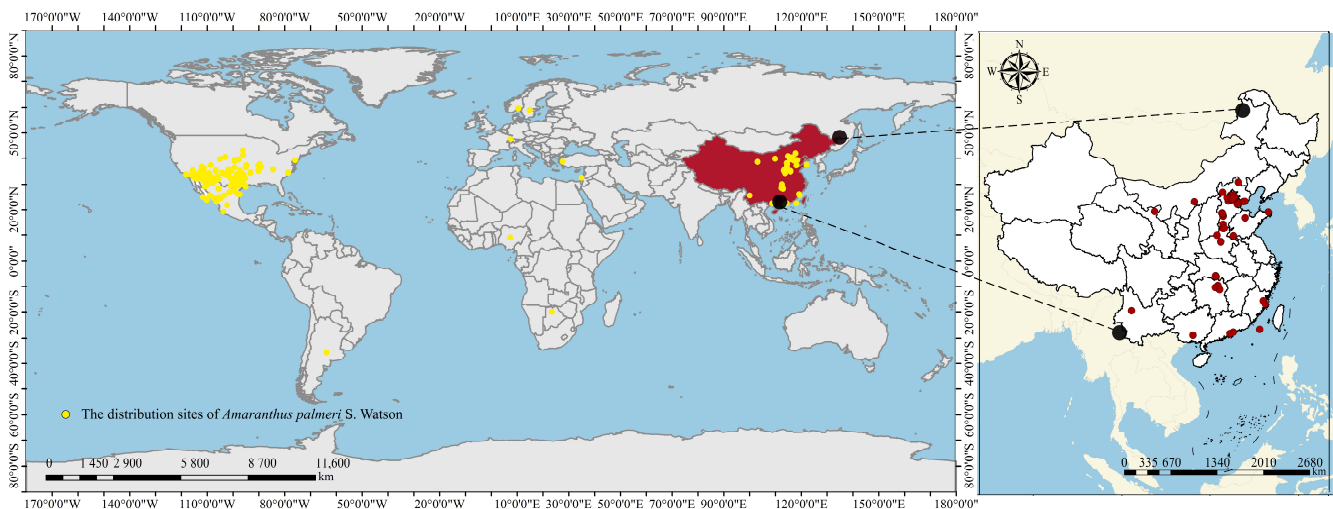

Figure 2. Distribution map of *Amaranthus palmeri*.

(2)   Environmental variables

The primary sources of the 53 environmental data utilized are as follows: 19 bioclimatic factors pertaining to the current climate, alongside elevation data, wind speeds, and bioclimatic factors linked to different future climate change scenarios, were acquired from the Worldclim dataset (https://worldclim.org/, accessed on 1 May 2023) [27]. The aforementioned environmental data exhibits an accuracy level of 2.5 arcmin. The future climate factor datasets were obtained from the Couple Model Intercomparison Project phase 6 (CMIP6) global change model BCC-CSM2-MR [28]. These datasets were selected based on the Shared Socioeconomic Pathway (SSP) scenarios, including the low forcing scenario SSP1-2.6, medium forcing scenario SSP2-4.5, and high forcing scenario SSP5-8.5. The timeframes considered were primarily focused on the 2021–2040 and 2041–2060 periods [29]. Meanwhile, 18 soil factors were selected from the Food and Agriculture Organization of the United Nations database 1.2 (https://www.fao.org/soils-portal/soil-survey/soil-maps-and-databases/harmonized-world-soil-database-v12/en/, accessed on 1 May 2023) [30]. Human footprint index V3 obtained from the Center for International Earth Science Information Network (ciesin.org) [31]. (Supplementary Table S1) The slope and aspect data were computed using the above elevation data within ArcGIS 10.8.2. To mitigate the risk of overfitting caused by multicollinearity among the environmental variables, the Pearson correlation analyses were conducted on the aforementioned set of 53 environmental factors using the ENMTools software 1.0. Moreover, the environmental factors were eliminated with a correlation coefficient ($|r|$) ≥ 0.8 and low contribution (Supplementary Tables S2 and S3, Figure S1). Furthermore, the jackknife was used to measure the importance of each variable in the model [32]. Subsequently, 25 environmental factors

both displaying statistically and biologically significant for the purpose of modeling were selected (Figure S2).

2.2. Invasive Historical Reconstruction of Amaranthus palmeri

The earliest time (1985) of occurrence records of *A. palmeri* in the CNKI and the CHV, was taken as the *A. palmeri* invasion onset year in China with the different county as the space unit and 10 years as the time slice. In addition, the records reported in the previous study were referred and were used to protract the historical spread distribution of *A. palmeri* in China from 1985–2022 using the ArcGIS 10.8.2 with the Mercator coordinate system (UTM 50 N) and the Geodetic System 1984 (WGS84) datum ellipsoid.

2.3. Construction, Optimization, and Evaluation of Models

The suitable geographic distribution changes of *A. palmeri* under current and future climate scenarios were predicted using the Maxent (V3.4.4) model. The two parameters, the regularization multiplier (RM) and feature combination (FC) in the Maxent model (V 3.4.4), were optimized using the ENMeval package 2.0 in the R language 3.6.3. A total set of 40 regularization multipliers (RM) ranging from 0.1 to 4.0, with an increment of 0.1, were employed in conjunction with 29 distinct feature combinations (FC). The FC included L (Linear), Q (Quadratic), T (Threshold), H (Fragmentation), P (Product), LQ, LP, LT, LH, QP, QT, QH, PT, PH, TH, LQP, LQT, LQH, LPT, LPH, QPT, QPH, QTH, LQPT, LQPH, LQTH, LPTH, and LQPTH. These parameters were cross-combined to facilitate a comprehensive evaluation using ENMtools 1.0. The aforementioned 1160 combinations were subsequently subjected to parameter tuning using the ENMeval package 2.0 for identification of the candidate model with delta. The AICc value of 0 was chosen as the optimal combination of parameters for the Maxent modeling process.

The distribution point data of *A. palmeri* in csv. format and the corresponding environmental data in asc. format were imported into Maxent (V3.4.4). The output format was configured to logistic. The test subset of the model consisted of 25% of the data, while the training subset of the model consisted of 75% of the data. We ran the MaxEnt model (V 3.4.4) 10 times (the average was considered the final result) and used the optimized cross-validation value of the FC and RM parameters, the "Random seed" option to enhance the model's randomness. The maximum iterations = 500, max number of background points = 10,000, convergence threshold = 0.00001, and prevalence = 0.5, were set to the default settings as suggested by previous studies [33,34].

The maximum training sensitivity plus specificity was chosen as the threshold (MTSPS) [35,36]. In addition, the MTSPS, considered simple and effective, was chosen to separate the final model's suitable and unsuitable areas for alien plants [37,38]. The potential geographical distribution of *A. palmeri* was classified into the following four categories under current and future climates: unsuitable $p \leq$ MTSPS; low suitability MTSPS $< p \leq 0.4$; medium suitability $0.4 < p \leq 0.6$; and high suitability $p > 0.6$.

The final model performance was evaluated with the area under the receiver operating characteristic (ROC) curve (AUC) and the true skill statistics (TSS). The AUC values span from 0 to 1.0 (higher values indicated a greater departure of the species distribution from a random distribution and a more accurate model). The evaluation index can be categorized into four levels based on the AUC values: invalid ($0 < $ AUC $ \leq 0.5$), poor ($0.5 < $ AUC $ \leq 0.7$), moderate ($0.7 < $ AUC $ \leq 0.9$), and high (AUC > 0.9). The TSS ranges from –1 to 1, the higher the values of TSS, the higher the accuracy of the model results [39].

2.4. Visualisation of Distribution Trends

The species distribution models (SDM) toolbox was used to calculate the changing trend of suitable areas using ArcGIS 10.8.2. First, the MTSS values were imported into ArcGIS 10.8.2, and the area of each change zone was calculated. ArcGIS 10.8.2 was used to identify seven climate change scenarios, including current, 2040s-SSP126, 2040s-SSP245, 2040s-SSP585, 2060s-SSP126, 2060s-SSP245, and 2060s-SSP585. The changes in the geometric

center of potentially suitable areas for *A. palmeri* under different periods were calculated based on SDM. Finally, the centroid in the risk area under a given set of conditions was compared with the changes in the centroid under different climatic conditions in each period, and the distance of the centroid shift was calculated.

3. Results

3.1. Model Performance

The cross-validation tuning with species distribution sites and environmental data in various combinations of RM and FC were conducted using the ENMeval package 1.0. The best model was chosen from a pool of 1160 candidate models (Supplementary Figure S3). When the values of FC and RM were separately set to PTH and 1.9, the minimum information criterion AICc was observed to be 0 (Table 1). Additionally, the average area under the curve (Avg. AUC) decreased by approximately 7.69%, while the mean odds ratio at 25% (Mean.OR$_{25}$) decreased by approximately 36.8% in comparison to the default parameters. These results suggested that the optimized parameters reduce the model complexity and improve the model fit. Hence, the parameters FC = PTH and RM = 1.9 were chosen to be utilized in the modeling process. The optimized model yielded an AUC value of 0.967 ± 0.00037, and a TSS value of 0.897, suggesting that the model exhibited a high level of accuracy in the predicting results (Supplementary Figure S4).

Table 1. Evaluation metrics of the Maxent model generated by ENMeval.

Type	FC	RM	Delta.AICc	Avg.diff.AUC	Mean.OR$_{25}$
default	LQPH	1	16.90	0.0065	0.076
optimized	PTH	1.9	0	0.006	0.048

3.2. Contribution of Key Environmental Factors

The key environmental factors impacting the geographical distribution of *A. palmeri* were identified using the Jackknife method and percent contribution, along with one-way response curves. Human activities, mean temperature of warmest quarter (Bio_10), wind speed in April (Wind_4), temperature seasonality (standard deviation × 100) (Bio_4), topsoil gravel content (T_gravel), and precipitation of warmest quarter (Bio_18) are main factors impacting on the distribution of *A. palmeri*. The cumulative contribution rate of six environmental factors accounted for over 85%. Additionally, the permutation importance was 80.2%, suggesting that these six factors played a significant role in shaping the distribution patterns of *A. palmeri* (Table 2).

Table 2. Key environment variables impacting the distribution of *A. palmeri*.

Variable	Percent Contribution (%)	Permutation Importance (%)
Human footprint	34.0	8.5
Bio_10	21.9	36.1
Wind_4	10.1	6.7
Bio_4	7.6	17.9
T_gravel	4.5	1.8
Bio_8	4.1	9.2

The one-way environmental curves indicated a positive correlation between the presence possibility of *A. palmeri* in suitable areas and the key environmental factors, such as human activities and wind speed in April respectively. It is easy for the establishment of *A. palmeri* when the human footprint index is higher than 10, and the Wind_4 is higher than 2.3 m/s (Figure 3a,c). Approximately 30 °C of Bio_10 and 1137 of Bio_4, was optimum to establish population for *A. palmeri* (Figure 3b,d). The range with the highest presence possibility of *A. palmeri* for the T_gravel was from 2.57–25.4%, however, when the T_gravel exceeded 25.4%, the presence possibility of *A.palmeri* decreased rapidly and below 0.5 in

areas with T_gravel approximately 25.6% (Figure 3e). The presence possibility of *A. palmeri* increased sharply when the Bio_18 was higher than 6 mm, stabilizing between 200 mm and 443 mm. However, when the Bio_18 reached 447 mm, the presence possibility of *A. palmeri* decreased temporarily and increased again at 456 mm. In regions with Bio_18 exceeded 1187.4 mm, the presence probability of the *A. palmeri* reached a peak (0.86) (Figure 3f).
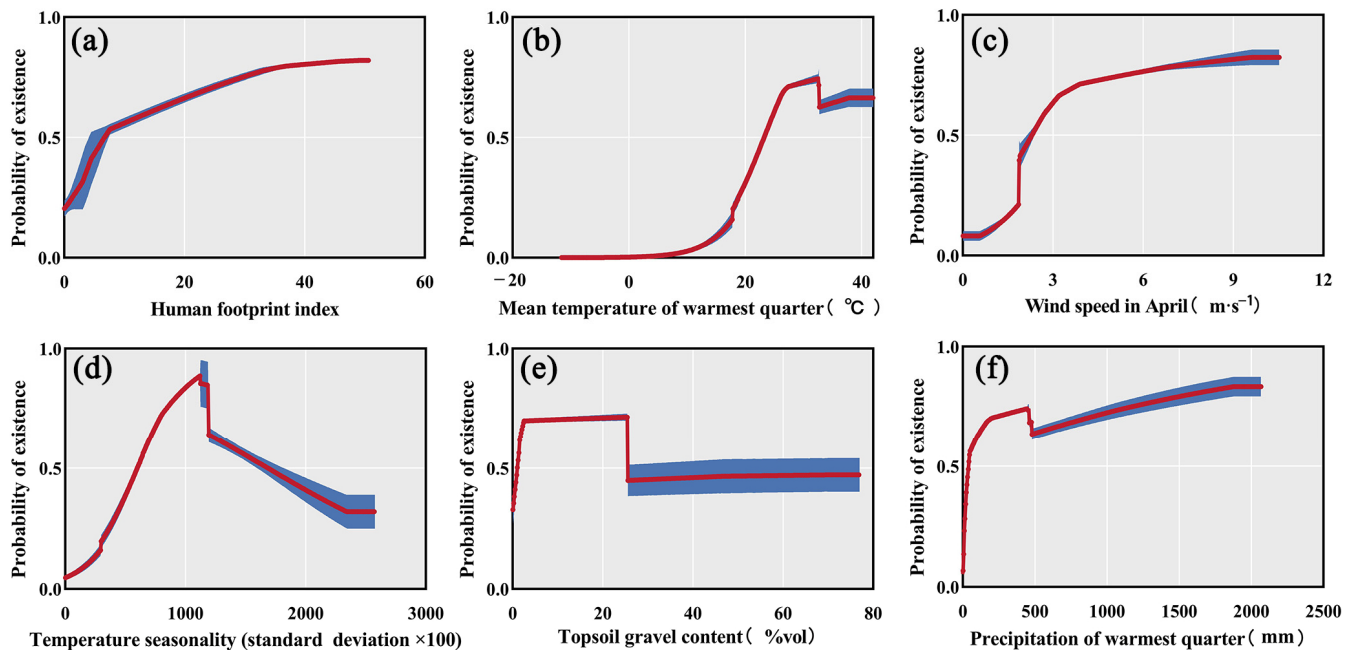

Figure 3. Response curves of Potential geographical distributions of *Amaranthus palmeri* under different environment factors. (**a**) Human footprint index (**b**) Mean temperature (**c**) Wind speed in April (**d**) Temperature seasonality (**e**) Topsoil gravel content (**f**) Precipitation of warmest quarter.

3.3. Historical Spread Dynamics of Amaranthus palmeri in China

The *A. palmeri* was first discovered in the village of Fan Zhuang zi in Fengtai District, Beijing in 1985. Subsequently, it was sporadically found in Beijing downtown before 1995 (Figure 4a). Since 1995, the distribution area of *A. palmeri* increased rapidly in Beijing downtown and spread to the suburban areas of Beijing. The diffusion rate was estimated to be 0.87 km per year from 1995 to 2005 (Figure 4b). The distribution area of *A. palmeri* experienced an explosive increase in the Beijing-Hebei-Tianjin region in 2015 and the spread rate reached 26.4 km per year (Figure 4c). Until 2022, the widespread distribution of *A. palmeri* was across numerous provinces, particularly in Beijing, Hebei, Tianjin, Henan, and Shandong. Occasional occurrences were also observed in provinces such as Hubei, Hunan, Sichuan, Fujian, and Guangxi. This spread pattern exhibited a notable invasion trend from north to south China (Figure 4d). Moreover, *A. palmeri* exhibited lag dissemination from 1985 to 1995 and then spread slowly from 1995 to 2005, and showed a notable acceleration in linear dissemination since 2005 (Figure 4e). Available information showed that the initial invasion sites of *A. palmeri* in China were primarily located along roadside areas. Our study revealed that approximately 34.5% of invasive locations of *A. palmeri* were situated adjacent to roadsides, followed by parks, foreshore, and proximity to processing plants (Figure 4f). Reconstruction of historical spread dynamics suggests that the invasion of *A. palmeri* in China originated in Beijing, followed by a subsequent expansion towards the southern regions. It exhibited a notable aggregation within the Beijing-Hebei-Tianjin region, and subsequently the distribution extended to the central and southern regions of China via transportation networks such as roads, railways, and rivers.
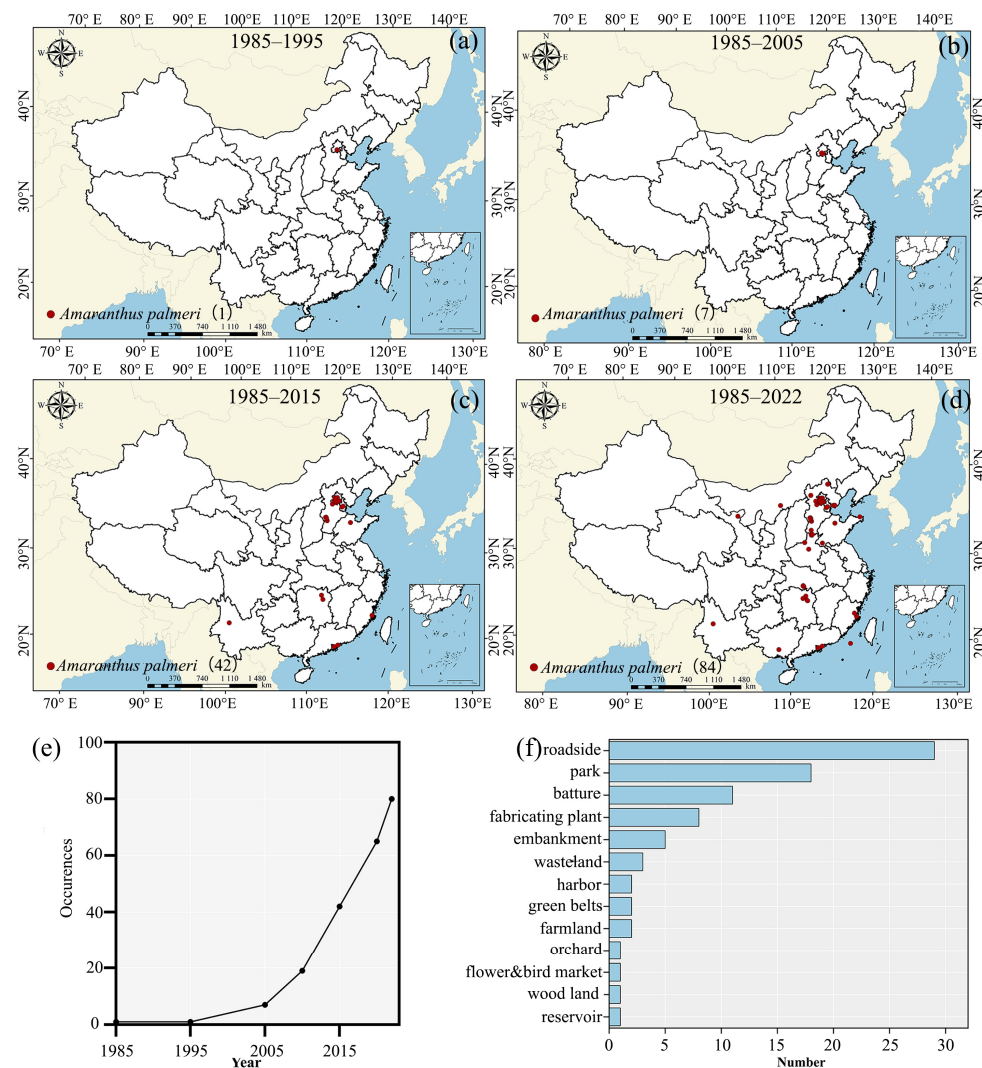
Figure 4. Reconstruction of historical spread dynamics of *Amaranthus palmeri* in China (**a**) *A. palmeri* distribution sites in 1985–1995 (**b**) *A. palmeri* distribution sites in 1985–2005 (**c**) *A. palmeri* distribution sites in 1985–2015 (**d**) *A. palmeri* distribution sites in 1985–2022 (**e**) The occurrence number of *A. palmeri* in the different year (**f**) The occurrence number in the different habitats.

3.4. Potential Geographical Distributions of Amaranthus palmeri in China

The mean MTSPS value was 0.1193 under the current climate environment. The current potential suitable habitat areas of *A. palmeri* were predicted to be located at the position of the geographic coordinates between 25°35′30″–36°6′0″ N and 105°56′0″–128°58′0″ E in China. The total potential geographical distribution areas reached 1,067,000 km^2, accounting for approximately 11.1% of the total land area of China. The highly potential suitable habitats reach 213,000 km^2 and are distributed in the northern regions of Beijing, Tianjin, southern Hebei Province, and northern Shandong Province, which correspond to the current geographical distribution of the *A. palmeri*. The medium potential suitable areas are distributed in Shanxi, Henan, Shaanxi, Anhui, Jiangsu, and Hubei provinces and reach 428,600 km^2, accounting for 40.2% of the total suitable area. However, only partial areas of Hunan, Jiangxi, Fujian, and Guangdong provinces are adaptive for *A. palmeri* (Figure 5a and Table 3). The potential suitable habitat areas of *A. palmeri* decreased gradually from north to south China under current climate scenarios.
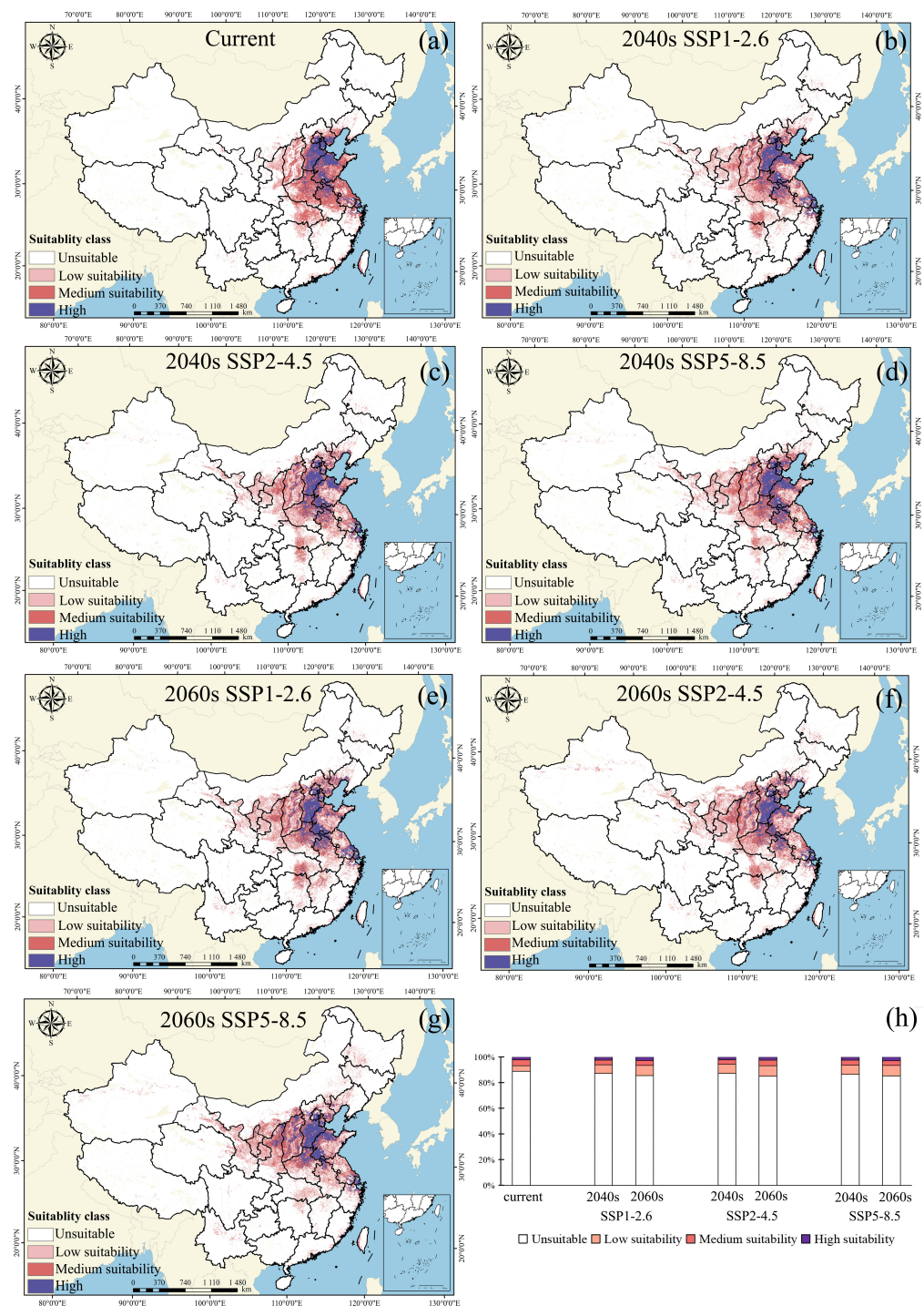
Figure 5. Potential suitability habitat area of *Amaranthus palmeri* in China (**a**) The potential geographical distributions of *A. palmeri* under the current scenarios (**b**) The potential geographical distributions of *A. palmeri* under the SSP1-2.6 in the 2040s (**c**) The potential geographical distributions of *A. palmeri* under the SSP2-4.5 in the 2040s (**d**) The potential geographical distributions of *A. palmeri* under the SSP5-8.5 in the 2040s (**e**) shows the potential geographical distributions of *A. palmeri* under the SSP1-2.6 in the 2060s (**f**) The potential geographical distributions of *A. palmeri* under the SSP2-4.5 in the 2060s (**g**) The potential geographical distributions of *A. palmeri* under the SSP5-8.5 in the 2060s (**h**) The change of suitable areas under the different scenarios.

Table 3. Potential suitable area of *A. palmeri* in 2040s under various carbon concentration emissions.

	Current	2040s SSP126	2040s SSP245	2040s SSP585
Unsuitable	853.2×10^4 km^2	837.0×10^4 km^2	837.4×10^4 km^2	831.4×10^4 km^2
Low suitability	42.5×10^4 km^2	65.8×10^4 km^2	68.3×10^4 km^2	67.8×10^4 km^2
Medium suitability	42.9×10^4 km^2	34.7×10^4 km^2	32.5×10^4 km^2	37.4×10^4 km^2
High suitability	21.3×10^4 km^2	22.5×10^4 km^2	21.8×10^4 km^2	23.5×10^4 km^2

The potentially suitable habitat areas of *A. palmeri* showed a notable expansion under future climate scenarios (Figure 5b–h). However, the future suitable habitat areas of *A. palmeri* showed a significant difference under different carbon emission scenarios (Figure 6a–f, Tables 3 and 4). Under SSP1-2.6, the total suitable areas accounted for 11.2% of the total land area of China in the period of 2022–2040. The lowly and highly suitable areas reached 658,100 and 225,000 km^2, respectively. Ningxia, Gansu, and Jiangxi provinces, as well as the northern Hunan Province, increase the suitability for the establishment of *A. palmeri*. Under SSP2-4.5, the total suitable habitat areas increased, but the suitability decreased compared to the current and SSP1-2.6 models. The medium potential suitable distribution in Henan, Hubei, and Shandong provinces are converted into low suitable distribution. Furthermore, the total area of medium-suitable habitats was reduced by 104,040 km^2. Under high forcing scenario SSP5-8.5, the total suitable area reached 1,285,900 km^2. The northern region of Anhui Province, Shanghai, as well as Xuzhou and Nantong of the Jiangsu province, become suitable for the establishment of *A. palmeri*.

Table 4. Potentially suitable area of *A. palmeri* in 2060s under various carbon concentration emissions.

	2060s SSP126	2060s SSP245	2060s SSP5.8
Unsuitable	821.1×10^4 km^2	815.9×10^4 km^2	818.0×10^4 km^2
Low suitability	76.6×10^4 km^2	80.0×10^4 km^2	78.2×10^4 km^2
Medium suitability	36.6×10^4 km^2	40.0×10^4 km^2	36.5×10^4 km^2
High suitability	25.7×10^4 km^2	24.3×10^4 km^2	27.3×10^4 km^2

Under SSP1-2.6, the total suitable areas expanded to approximately 445,000 km^2 in the 2040–2060 periods. The potential geographical distributions extended to Erdos City in Inner Mongolia, eastern Gansu Province, the eastern region (such as Qingyang City, Lanzhou City, Baiyin City, Zhangye City) of Gansu Province, and the Ningxia Hui Autonomous region. Under SSP2-4.5, the total potential suitable area was the largest at approximately 1,441,100 km^2. Although the medium suitable areas decreased, both the lowly suitable and highly suitable areas increased significantly (Table 5). Under SSP5-8.5, the highly suitable areas showed an obvious increase and reached 272,800 km^2. The potential suitable zones extended to Haidong City in Qinghai Province and Jiayuguan City in Gansu Province.

Table 5. Potential suitability habitat area transfer of *Amaranthus palmeri* under different climatic scenarios.

	2040-2.6	2040-4.5	2040-5.8	2060-2.6	2060-4.5	2060-5.8
Increased	26.7×10^4 km^2	30.5×10^4 km^2	33.8×10^4 km^2	44.5×10^4 km^2	51.6×10^4 km^2	53.6×10^4 km^2
served	98.7×10^4 km^2	92.2×10^4 km^2	94.8×10^4 km^2	94.4×10^4 km^2	92.5×10^4 km^2	88.3×10^4 km^2
Lost	10.9×10^4 km^2	14.6×10^4 km^2	12.0×10^4 km^2	12.4×10^4 km^2	14.3×10^4 km^2	18.4×10^4 km^2

Comparing the potential geographical distributions of *A. palmeri* under the current and future climate scenarios, Beijing, Hebei, Tianjin, the northern Anhui Province, northern Jiangsu Province, and Shanghai, are potential areas of highly suitable habitats for *A. palmeri*. The potential geographical distributions of *A. palmeri* gradually extended to southern Inner Mongolia, eastern Kansu Province, and Ningxia. The area of suitable habitats in eastern

Hubei and western Jiangxi province decreased gradually and part of them disappeared until the 2060s.
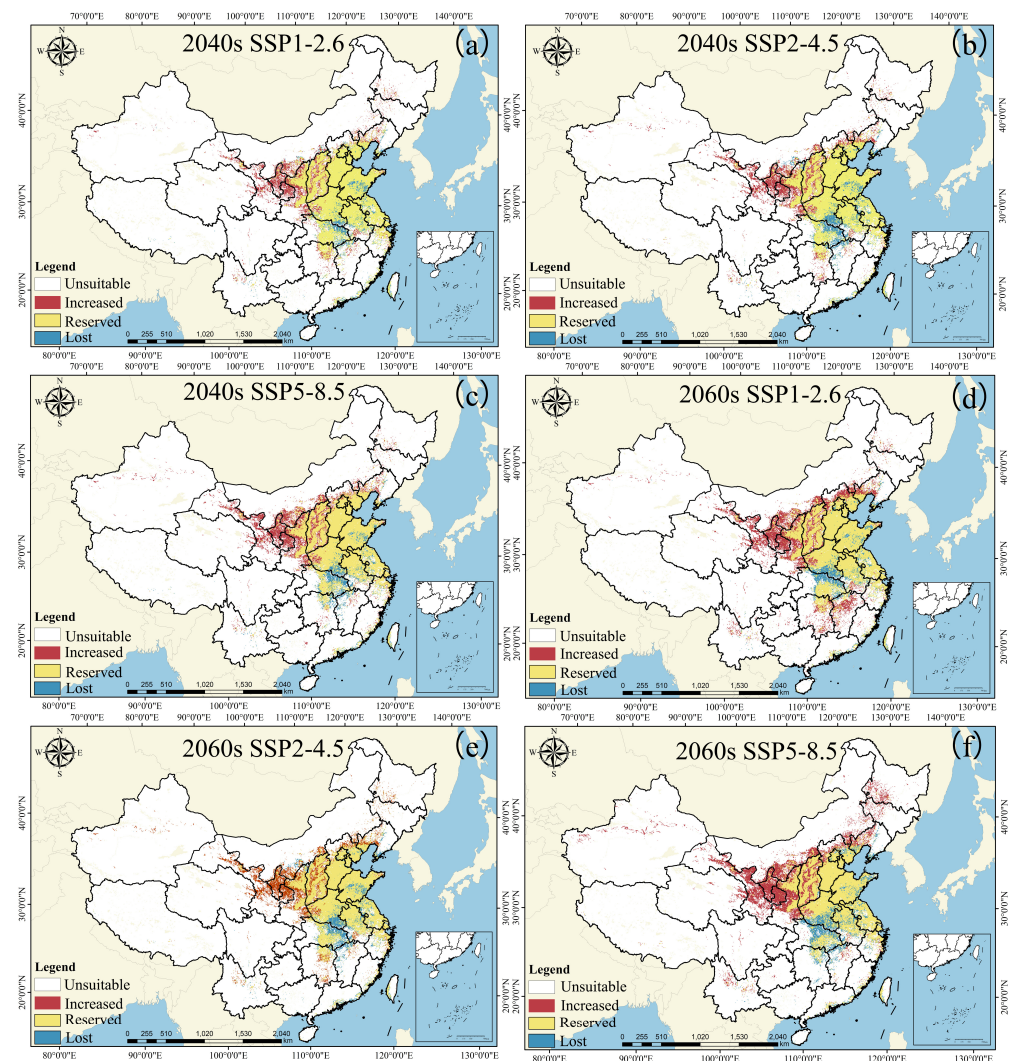

Figure 6. Potential suitability habitat area transfer of *Amaranthus palmeri* under different climatic scenarios (**a**) The potential suitability habitat areas transfer under the 2040s SSP1-2.6 (**b**) The potential suitability habitat areas transfer under the 2040s SSP2-4.5 (**c**) The potential suitability habitat areas transfer under the 2040s SSP5-8.5 (**d**) The potential suitability habitat areas transfer under the 2060s SSP1-2.6 (**e**) The potential suitability habitat areas transfer under the 2060s SSP2-4.5 (**f**) The potential suitability habitat areas transfer under the 2060s SSP5-8.5.

3.5. The Centroid Distribution Transfer of Amaranthus palmeri under Different Climatic Scenarios

Under current climate scenarios, the centroid of suitable habitat of *A. palmeri* was at the position of (115°30′38″ E, 34°49′44″ N) in the Caoxian County, Heze City, Shandong Province (Figure 7). However, under three future climate scenarios, the suitable habitats of *A. palmeri* extended to northwest China but showed a certain difference in distances. Under SSP1-2.6, the centroid of suitable habitat of *A. palmeri* would shift to (114°10′49″ E, 35°25′9″ N) in the Weihui City, Henan Province in the 2040s, which northwestward extended approximately 136.24 km from the current position. Moreover, the centroid would shift to (113°44′27″ E, 35°37′56″ N) in the Huixian City, Henan Province in the 2060s, which northwestward extended approximately 182.43 km from the current position. Under SSP2-4.5, the centroid would shift to (113°54′23″ E, 35°45′27″ N) in Linzhou City, Henan Province in the 2040s, which northwestward extended approximately 177.59 km from the current position. In addition, the centroid would shift to (113°5′57″ E, 36°20′57″ N)

in Luzhou District, Changzhi City, Shanxi Province in the 2060s, which northwestward extended 97.83 km from the current position. Under SSP5-8.5, the centroid would shift to (113°46′52″ E, 35°52′57″ N) in the 2040s in Linzhou City, Anyang City, Henan Province, which northwestward extended approximately 194.93 km from the current position. Moreover, the centroid would shift to (113°7′10″ E, 36°22′44″ N) in the 2060s in Lucheng District, Changzhi City, Shanxi Province, which northwestward extended approximately 275.97 km from the current position.
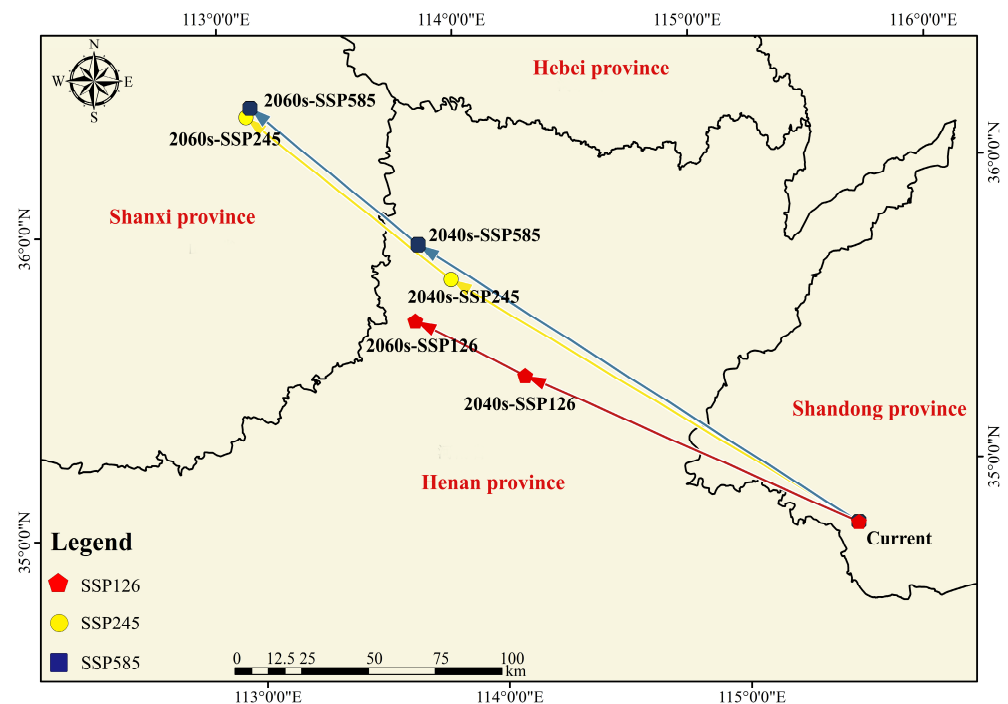

Figure 7. The trend of centroid distribution transfer of *Amaranthus palmeri*.

4. Discussion

4.1. Invasive Historical Reconstruction and Key Driver

Invasion processes of non-native plants in novel environments include lag, acceleration, and stable phases [40,41] Previous studies have revealed a significantly linear relationship between the range size of invasive plants and residence time [42,43]. Aikio found that nearly all the New Zealand weed species had a lag-phase, which averaged around 20−30 years, with 4% of species having a lag-phase greater than 40 years [44]. In a statistical analysis estimating lag times for perennial *Ageratina adenophora* introduced to China, the time between introduction and first spread was estimated at 20 years [45]. The invasive historical reconstruction of *A. palmeri*, showed that species occurrence increased slowly over 10 years after it invaded China, followed by a population outbreak in 2005a. It has a shorter lag phase compared with *A. adenophora*. It is possibly due to annual/biennial alien plant species that can disperse faster than perennial species because of higher population growth rates and shorter life cycles [40,46]. Short-life-history species generally have a faster evolutionary rate than long-life-history species, given that they require less time to reach maturity and to reproduce [47]. In addition, the high plasticity, rapid growth potential, high photosynthetic rates, early season germination behavior, and property of diaheliotropism of *A. palmeri*, all of which allow it to accumulate biomass at a faster rate than surrounding species and contribute to its widespread. [25,48].

Furthermore, *A. palmeri* seeds and fragments are commonly dispersed via wind (anemochory) and human-induced actions (anthropochory) [49,50], its pollen can move long distance [50], which significantly shorten its lag times. Our study found that human activities were the most critical environmental factor for the distribution patterns of *A. palmeri*,

and the wind speed came later (took third place). It is often argued that habitat degradation and anthropogenically driven disturbance can facilitate the successful establishment of invasive taxa [51]. Previous studies showed that in the process of urbanization, exotic plants have been widely introduced [52], urban areas contain more alien plants compared to rural areas, and non-native species are positively associated with urbanization. [53,54]. In 1978a, Chinese reform and opening up policy prompted the rate of urban expansion to accelerate until 1990a, when it reached its first peak with an annual expansion rate of 1171.27 km^2 [55]. The urban expansion rate ascended to an average of 1817.89 km^2 per year in 2010–2018, an overall faster rate compared to that of 2000–2010 [55]. Our study found that *A. palmeri* expanded at a rate of 26.4 km per year in China from 2010–2015, which is much higher than that from 2000–2010. This expanded rate is consistent with the pace of urbanization. Another study indicated that the niche width of non-native plants increases with human activities and human activities directly or indirectly affect the invasion process [56,57]. In our results, the value of human footprint index increased concomitantly with the probability increase of the species presence, revealing that human activities played an important role and possibly influenced the geographical distribution of *A. palmeri*. The result is similar with the potential geographical distribution of non-invasive plants reported by Yang et al. [35].

Temperature, precipitation, human activities, and wind speed were key environmental variables for *A. palmeri* growth. According to its region of origin, *A. palmeri* is well adapted to growth under regimes of high temperature and low rainfall [58]. Our study suggested that the suitable areas of *A. palmeri* are distributed predominantly in northern China, much more than the coastal province. These areas are characterized by a monsoonal continental climate with cold dry winters and warm wet summers [59]. This is probably due to the climate in northern China being very similar to the area of the origin of *A. palmeri*. On the other hand, *A. Palmeri* germinated faster at higher latitudes. Seeds from lower latitudes tended to have lower and slower germination rates, the germination rate and index increased linearly with latitude [14,60]. In addition, *A. palmeri* were stunted, growth was generally slow and no seed germination was observed at 10−15 °C, indicating it responds negatively to low temperatures [61]. Moreover, *A. palmeri* will germinate when soil average temperatures are greater than 25 °C [25]. Seed germination increased gradually as temperature increased and peaked at 30–35 °C. The root activity increased in *A. palmeri* when temperature increased to 30–35 °C. In general, its seed germination declined at temperatures above 30–35 °C [62]. Ledda et al. suggested that soil water could induce germination and seeds can germinate over a wide range of temperatures without water restrictions [58]. Furthermore, the growth and fecundity of *A. palmeri* decreased with the soil water stress increased, and water stress could reduce the height of *A. palmeri* [63,64]. We also found that the growth and fecundity of *A. palmeri* were affected by the optimal range of the mean temperature of the warmest quarter and precipitation of the warmest quarter. These data suggested that the continuous high temperatures and frequent precipitation in low-latitude regions (southern China) could restrict establishment of *A. palmeri*.

4.2. Potential Geographical Distributions under Climate Change

Aside from the widely known effect of human activities on the spread and success of invasive taxa, it is often argued that temperature increases have significantly affected the distribution of invasive plants [65]. For example, the potential geographical distributions of Ambrosia species, are expected to expand under climate change in the Anthropocene [66]. In China, the future potential distributions of *Lolium temulentum* are predicted to expand under climate change scenarios [35]. Our predictions suggested that the potential geographical distributions of *A. palmeri* will expand and continue to spread northwestern in the 2040s and 2060s when temperature increases under future climate scenarios (SSP1-2.6, SSP2-4.5, SSP5-8.5). As a C$_4$ plant, *A. palmeri* can maintain a high photosynthetic capacity and growth under water stress conditions using osmotic adjustment to increase leaf solute concentration, allowing the stomata to remain open longer during conditions of water

stress and maintain CO_2 diffusion to chloroplasts [63]. In addition, *A. palmeri* exhibits high plasticity and genetic variation between populations for multiple life-history traits [67]. The correlation between phenotypic variation and temperature in different latitude populations of *A. palmeri* shows strong climate adaptability [14]. Under scenarios of warmer regional temperatures, seeds at higher latitudes could germinate earlier and have a higher germination rate, which would favor a potential northern expansion of this invasive plant [60]. It is therefore likely that *A. palmeri* may evolve to better adapt to changing environments, thus facilitating its expansion into new areas [68].

Previous studies suggested that the niche of invasive plants was not always strictly conserved. Invasive plants would tend to shift their ranges with climate change. Thus all directions around the invasive plants will face the risk of potential future invasion [69,70]. Our data showed that the centroid of *A. palmeri* will transfer to the northwest and to different provinces under the future scenarios, which suggested a high adaptability to new habitats and climate change since its invasion in China and tends to spread in all directions at a high speed.

4.3. Prevention and Control of Amaranthus palmeri in China

Whilst herbicide application is the most common method of weed control, recent research suggests that *A. palmeri* has a proclivity to develop herbicide resistance [9,25]. In addition, *A. palmeri* plants are capable of quick regrowth under various cutting treatments. Simply severing *A. palmeri* stems as a means of removal, instead of uprooting the entire plant, may allow a significant portion of *A. palmeri* to regrow and produce seed [25,71]. Thus, one of the most useful methods to prevent the future spread and impact of *A. palmeri* is the development of early detection and proactive response protocols [25,72]. We demonstrated that the current overlap of *A. palmeri* is mainly distributed in Beijing, Hebei, Tianjin, Henan, Shandong, Shanxi, Shaanxi, Shanghai, northern Anhui, Hubei, and northern Jiangsu. The invasion is predicted to be more intense in Beijing, Tianjin, and Hebei. Shanxi, Shaanxi, and Ningxia were predicted to be novel environments that exist at medium invasive risk for *A. palmeri*. It is also significant that revegetation programs after successful eradication of *A. palmeri* in the invaded area must be implemented to restore native vegetation and prevent secondary invasions [73]. Based on the simulation results and the characteristics of *A. palmeri*, we can propose some recommendations to effectively control this species. We propose that early detection and warning should be established in northwestern and northern China, especially in Shaanxi, Shanxi, and Ningxia. Moreover, we advocate for the establishment of priority management areas in regions close to the conduit of *A. palmeri* seed transport such as railways, roads, and riverbanks. For the invaded area, considering the high cost and inefficiency of manual and mechanical control, and the limitation of chemical control to cause environmental pollution, biological and ecological control techniques should be adopted to prevent its colonization and dispersal. Additionally, the government should create an invasive species information database to improve information exchange and sharing between regions, allowing for timely invasion prediction, risk assessment, and emergency prevention and control measures to prevent the predicted proliferation from becoming a reality [32]. Although our data suggests that *A. palmeri* could not severely invade the ecoregions listed in southern Inner Mongolia and eastern Gansu, we need to prevent the escalated risk of *A. palmeri* by extreme climatic events in these ecoregions.

4.4. Research Significance and Prospect

In our study, the Maxent model (V 3.4.4) achieved a high mean accuracy (AUC = 0.967, TSS = 0.897). The invasive history of *A. palmeri* has been reconstructed. Moreover, the key environmental variables affecting the suitability habitat of *A. palmeri* were determined and the potentially suitable areas in China under current and future climate scenarios were predicted, which provides a basis for early warning and combined management. However, our study still has some deficiencies. Temporal and geographical biases can exist in herbarium collections because of irregular collecting intensity. In addition, a geographical bias might

be present as a result of different levels of collecting intensity [74,75]. The sampling bias will naturally affect the results in the Maxent model [76]. Moreover, *A. palmeri* distribution is constrained by vegetation dynamics, inter-specific competition, and heterogeneity. In the near future, it is necessary to carry out a field survey on risk areas and use updated data combined with more variables to conduct further regional scale analysis based on the ensemble model.

5. Conclusions

In this study, the invasive history and distribution patterns of *A. palmeri* from 1985 to 2022 in China were reconstructed, and then the potential geographical distribution of *A. palmeri* was predicted under current and future (SSP1-2.6, SSP2-4.5, SSP5-8.5) climate scenarios using the optimal MaxEnt model (V 3.4.4) and ArcGIS 10.8.2. Under the future scenarios, the highly suitable habitats of *A. palemri* showed an increasing trend, mainly distributed in Beijing, Tianjin, and Hebei. The centroid distribution would northwestward extend under future climate scenarios. Most importantly, the human footprint index, mean temperature of the warmest quarter (Bio_10), April wind speed (Wind_4), temperature seasonality (standard deviation × 100) (bio_4), topsoil gravel content (T_gravel), and precipitation of the warmest quarter (Bio_18) were key environmental factors affecting distribution and growth of *A. palmeri*. However, the effects of other factors cannot be ignored, such as vegetation dynamics, inter-specific competition, and heterogeneity. In the future, it is necessary to carry out a field survey on risk areas and use updated data combined with more variables to conduct further regional scale analysis based on the ensemble model. Based on the current state of technology, our study achieved a high mean accuracy (AUC = 0.967, TSS = 0.897), the results of our study will also help in developing effective strategies for the early warning, preventive, control, and management of *A. palmeri* in China.

Supplementary Materials: The following supporting information can be downloaded at: https://www.mdpi.com/article/10.3390/agronomy13102498/s1. Tables S1. Species data and environmental variables source. Table S2. Environmental variables for the potential geographical distribution of *Amaranthus palmeri*. Table S3. The Pearson correlation coefficient of bioclimatic variables. Figure S1. Relation between 53 environmental variables. Figure S2. Importance of environmental variables of *Amaranthus palmeri* by "Jackknife method". Figure S3. The best model was chosen from a pool of 1160 candidate models. Figure S4. The MaxEnt model calibration and AUC of *Amaranthus palmeri*.

Author Contributions: X.J., writing—original draft preparation; M.L., J.L. and Q.Y., methodology; Z.L., writing—review and editing, supervision. All authors have read and agreed to the published version of the manuscript.

Data Availability Statement: All data generated or analyzed during this study are included in this published article.

Conflicts of Interest: The authors declare no conflict of interest.

References

1. Sherpa, S.; Despres, L. The evolutionary dynamics of biological invasions: A multi-approach perspective. *Evol. Appl.* **2021**, *14*, 1463–1484. [CrossRef]
2. Diagne, C.; Leroy, B.; Vaissiere, A.C.; Gozlan, R.E.; Roiz, D.; Jaric, I.; Salles, J.M.; Bradshaw, C.J.A.; Courchamp, F. High and rising economic costs of biological invasions worldwide. *Nature* **2021**, *592*, 571–576. [CrossRef]
3. Diagne, C.; Leroy, B.; Gozlan, R.E.; Vaissiere, A.C.; Assailly, C.; Nuninger, L.; Roiz, D.; Jourdain, F.; Jaric, I.; Courchamp, F. InvaCost, a public database of the economic costs of biological invasions worldwide. *Sci. Data* **2020**, *7*, 277. [CrossRef] [PubMed]
4. Pysek, P.; Richardson, D.M.; Gadgil, A.; Liverman, D.M. Invasive Species, Environmental Change and Management, and Health. *Annu. Rev. Environ. Resour.* **2010**, *35*, 25–55. [CrossRef]
5. Buchadas, A.; Vaz, A.S.; Honrado, J.P.; Alagador, D.; Bastos, R.; Cabral, J.A.; Santos, M.; Vicente, J.R. Dynamic models in research and management of biological invasions. *J. Environ. Manag.* **2017**, *196*, 594–606. [CrossRef] [PubMed]

6. Barco-Antonanzas, M.; Gil-Monreal, M.; Eceiza, M.V.; Royuela, M.; Zabalza, A. Primary metabolism in an *Amaranthus palmeri* population with multiple resistance to glyphosate and pyrithiobac herbicides. *Plant. Sci.* **2022**, *318*, 111212. [CrossRef] [PubMed]
7. Bobadilla, L.K.; Baek, Y.; Tranel, P.J. Comparative transcriptomic analysis of male and females in the dioecious weeds *Amaranthus palmeri* and Amaranthus tuberculatus. *BMC Plant Biol.* **2023**, *23*, 339. [CrossRef]
8. Matzrafi, M.; Herrmann, I.; Nansen, C.; Kliper, T.; Zait, Y.; Ignat, T.; Siso, D.; Rubin, B.; Karnieli, A.; Eizenberg, H. Hyperspectral Technologies for Assessing Seed Germination and Trifloxysulfuron-methyl Response in *Amaranthus palmeri* (Palmer Amaranth). *Front. Plant Sci.* **2017**, *8*, 474. [CrossRef]
9. Cao, J.J.; Wu, Q.M.; Wan, F.H.; Guo, J.Y.; Wang, R. Reliable and rapid identification of glyphosate-resistance in the invasive weed *Amaranthus palmeri* in China. *Pest Manag. Sci.* **2022**, *78*, 2173–2182. [CrossRef]
10. Singh, V.; Dou, T.Y.; Krimmer, M.; Singh, S.; Humpal, D.; Payne, W.Z.; Sanchez, L.; Voronine, D.V.; Prosvirin, A.; Scully, M.; et al. Raman Spectroscopy Can Distinguish Glyphosate-Susceptible and -Resistant Palmer Amaranth (*Amaranthus palmeri*). *Front. Plant Sci.* **2021**, *12*, 657963. [CrossRef]
11. Mesgaran, M.B.; Matzrafi, M.; Ohadi, S. Sex dimorphism in dioecious Palmer amaranth (*Amaranthus palmeri*) in response to water stress. *Planta* **2021**, *254*, 17. [CrossRef] [PubMed]
12. Gaines, T.A.; Ward, S.M.; Bukun, B.; Preston, C.; Leach, J.E.; Westra, P. Interspecific hybridization transfers a previously unknown glyphosate resistance mechanism in *Amaranthus* species. *Evol. Appl.* **2012**, *5*, 29–38. [CrossRef] [PubMed]
13. Montgomery, J.S.; Giacomini, D.; Waithaka, B.; Lanz, C.; Murphy, B.P.; Campe, R.; Lerchl, J.; Landes, A.; Gatzmann, F.; Janssen, A.; et al. Draft Genomes of *Amaranthus tuberculatus*, *Amaranthus hybridus*, and *Amaranthus palmeri*. *Genome Biol. Evol.* **2020**, *12*, 1988–1993. [CrossRef] [PubMed]
14. Zhang, X.Y.; Zhao, J.; Wang, M.M.; Li, Z.P.; Lin, S.; Chen, H. Potential distribution prediction of *Amaranthus palmeri* S. Watson in China under current and future climate scenarios. *Ecol. Evol.* **2022**, *12*, 9505. [CrossRef] [PubMed]
15. Seebens, H.; Essl, F.; Dawson, W.; Fuentes, N.; Moser, D.; Pergl, J.; Pysek, P.; van Kleunen, M.; Weber, E.; Winter, M.; et al. Global trade will accelerate plant invasions in emerging economies under climate change. *Glob. Chang. Biol.* **2015**, *21*, 4128–4140. [CrossRef] [PubMed]
16. Zhang, M.; Shi, C.; Li, X.Y.; Wang, K.F.; Qiu, Z.L.; Shi, F.C. Changes in the structure and function of rhizosphere soil microbial communities induced by *Amaranthus palmeri* invasion. *Front. Microbiol.* **2023**, *14*, 1114388. [CrossRef]
17. Jarnevich, C.S.; Holcombe, T.R.; Barnett, D.T.; Stohlgren, T.J.; Kartesz, J.T. Forecasting Weed Distributions using Climate Data: A GIS Early Warning Tool. *Invasive Plant Sci. Manag.* **2010**, *3*, 365–375. [CrossRef]
18. Paulus, M.; Teubner, D.; Hochkirch, A.; Veith, M. Journey into the past: Using cryogenically stored samples to reconstruct the invasion history of the quagga mussel (*Dreissena rostriformis*) in German river systems. *Biol. Invasions* **2014**, *16*, 2591–2597. [CrossRef]
19. Vallejo-Marin, M.; Friedman, J.; Twyford, A.D.; Lepais, O.; Ickert-Bond, S.M.; Streisfeld, M.A.; Yant, L.; van Kleunen, M.; Rotter, M.C.; Puzey, J.R. Population genomic and historical analysis suggests a global invasion by bridgehead processes in *Mimulus guttatus*. *Commun. Biol.* **2021**, *4*, 327. [CrossRef]
20. Capinha, C.; Seebens, H.; Cassey, P.; Garcia-Diaz, P.; Lenzner, B.; Mang, T.; Moser, D.; Pysek, P.; Rodder, D.; Scalera, R.; et al. Diversity, biogeography and the global flows of alien amphibians and reptiles. *Divers. Distrib.* **2017**, *23*, 1313–1322. [CrossRef]
21. Duncan, R.P.; Blackburn, T.M.; Rossinelli, S.; Bacher, S. Quantifying invasion risk: The relationship between establishment probability and founding population size. *Methods Ecol. Evol.* **2014**, *5*, 1255–1263. [CrossRef]
22. Dyer, E.E.; Cassey, P.; Redding, D.W.; Collen, B.; Franks, V.; Gaston, K.J.; Jones, K.E.; Kark, S.; Orme, C.D.L.; Blackburn, T.M. The global distribution and drivers of alien bird species richness. *PLoS Biol.* **2017**, *15*, e2000942. [CrossRef] [PubMed]
23. Briscoe Runquist, R.D.; Lake, T.; Tiffin, P.; Moeller, D.A. Species distribution models throughout the invasion history of Palmer amaranth predict regions at risk of future invasion and reveal challenges with modeling rapidly shifting geographic ranges. *Sci. Rep.* **2019**, *9*, 2426. [CrossRef] [PubMed]
24. Kistner, E.J.; Hatfield, J.L. Potential geographic distribution of Palmer amaranth under current and future climates. *Arg. Env. Lett.* **2018**, *3*, 170044. [CrossRef]
25. Roberts, J.; Florentine, S. A review of the biology, distribution patterns and management of the invasive species *Amaranthus palmeri* S. Watson (Palmer amaranth): Current and future management challenges. *Weed Res.* **2022**, *62*, 113–122. [CrossRef]
26. Yang, J.; Hu, Q.; You, L.; Cai, Z.; Chen, Y.; Wei, H.; Xu, Z.; He, Z.; Yin, G.; Xu, B. Mapping the potential northern limits and promotion extent of ratoon rice in China. *Appl. Geogr.* **2023**, *150*, 102822. [CrossRef]
27. Fick, S.E.; Hijmans, R.J. WorldClim 2: New 1-km spatial resolution climate surfaces for global land areas. *Int. J. Climatol.* **2017**, *37*, 4302–4315. [CrossRef]
28. Eyring, V.; Bony, S.; Meehl, G.A.; Senior, C.A.; Stevens, B.; Stouffer, R.J.; Taylor, K.E. Overview of the Coupled Model Intercomparison Project Phase 6 (CMIP6) experimental design and organization. *GeoSci. Model. Dev.* **2016**, *9*, 1937–1958. [CrossRef]
29. Petrie, R.; Denvil, S.; Ames, S.; Levavasseur, G.; Fiore, S.; Allen, C.; Antonio, F.; Berger, K.; Bretonniere, P.A.; Cinquini, L.; et al. Coordinating an operational data distribution network for CMIP6 data. *Geosci. Model. Dev.* **2021**, *14*, 629–644. [CrossRef]
30. Fischer, G.; Nachtergaele, F.; Prieler, S.; Teixeira, E.I.; Toth, G.; Velthuizen, H.V.; Verelst, L.; Wiberg, D. *Global Agro-Ecological Zones (GAEZ v3.0)*; International Institute for Applied Systems Analysis: Laxenburg, Austria, 2012.
31. Venter, O.; Sanderson, E.W.; Magrach, A.; Allan, J.R.; Beher, J.; Jones, K.R.; Possingham, H.P.; Laurance, W.F.; Wood, P.; Fekete, B.M.; et al. *Last of the Wild Project, Version 3 (LWP-3): 2009 Human Footprint, 2018 Release*; NASA: Washington, DC, USA, 2018.

32. Xu, Y.; Ye, X.; Yang, Q.; Weng, H.; Liu, Y.; Ahmad, S.; Zhang, G.; Huang, Q.; Zhang, T.; Liu, B. Ecological niche shifts affect the potential invasive risk of *Phytolacca americana* (Phytolaccaceae) in China. *Ecol. Process.* **2023**, *12*, 1. [CrossRef]

33. Lin, J.; Li, H.; Zeng, Y.; He, X.; Zhuang, Y.; Liang, Y.; Lu, S. Estimating potential illegal land development in conservation areas based on a presence-only model. *J. Environ. Manag.* **2022**, *321*, 115994. [CrossRef]

34. Khosa, D.; Marr, S.M.; Wasserman, R.J.; Zengeya, T.A.; Weyl, O.L. An evaluation of the current extent and potential spread of Black Bass invasions in South Africa. *Biol. Invasions* **2019**, *21*, 1721–1736. [CrossRef]

35. Yang, M.; Zhao, H.X.; Xian, X.Q.; Wang, R.; Yang, N.W.; Chen, L.; Liu, W.X. Assessing risk from invasive alien plants in China: Reconstructing invasion history and estimating distribution patterns of *Lolium temulentum* and *Aegilops tauschii*. *Front. Plant Sci.* **2023**, *14*, 1113567. [CrossRef]

36. Zahoor, B.; Liu, X.; Songer, M. The impact of climate change on three indicator Galliformes species in the northern highlands of Pakistan. *Environ. Pollut.* **2022**, *29*, 54330–54347. [CrossRef] [PubMed]

37. Aidoo, O.F.; Souza, P.G.C.; da Silva, R.S.; Santana, P.A.; Picanco, M.C.; Kyerematen, R.; Setamou, M.; Ekesi, S.; Borgemeister, C. Climate-induced range shifts of invasive species (*Diaphorina citri* Kuwayama). *Pest Manag. Sci.* **2022**, *78*, 2534–2549. [CrossRef] [PubMed]

38. Ramos, R.S.; Kumar, L.; Shabani, F.; Picanco, M.C. Risk of spread of tomato yellow leaf curl virus (TYLCV) in tomato crops under various climate change scenarios. *Agric. Syst.* **2019**, *173*, 524–535. [CrossRef]

39. Xian, X.; Zhao, H.; Wang, R.; Huang, H.; Chen, B.; Zhang, G.; Liu, W.; Wan, F. Climate change has increased the global threats posed by three ragweeds (*Ambrosia* L.) in the Anthropocene. *Sci. Total Environ.* **2023**, *859*, 160252. [CrossRef] [PubMed]

40. Ni, M. Herbarium records reveal multiple phases in the relationship between minimum residence time and invasion ranges of alien plant species. *Plants People Planet* **2023**, *5*, 47–57. [CrossRef]

41. Shigesada, N.; Kawasaki, K. Invasion and the range expansion of species: Effects of long-distance dispersal. *Dispersal Ecol.* **2002**, *17*, 350–373.

42. Sheppard, C.S.; Schurr, F.M. Biotic resistance or introduction bias? Immigrant plant performance decreases with residence times over millennia. *Glob. Ecol. Biogeogr.* **2019**, *28*, 222–237. [CrossRef]

43. Dyer, E.E.; Franks, V.; Cassey, P.; Collen, B.; Cope, R.C.; Jones, K.E.; Sekercioglu, C.H.; Blackburn, T.M. A global analysis of the determinants of alien geographical range size in birds. *Glob. Ecol. Biogeogr.* **2016**, *25*, 1346–1355. [CrossRef]

44. Aikio, S.; Duncan, R.P.; Hulme, P.E. Lag-phases in alien plant invasions: Separating the facts from the artefacts. *Oikos* **2010**, *119*, 370–378. [CrossRef]

45. Wang, R.; Wang, Y.Z. Invasion dynamics and potential spread of the invasive alien plant species *Ageratina adenophora* (Asteraceae) in China. *Divers. Distrib.* **2006**, *12*, 397–408. [CrossRef]

46. Huang, Q.Q.; Qian, C.; Wang, Y.; Jia, X.; Dai, X.F.; Zhang, H.; He, F.; Peng, S.L.; Wang, G.X. Determinants of the geographical extent of invasive plants in China: Effects of biogeographical origin, life cycle and time since introduction. *Biodivers. Conserv.* **2010**, *19*, 1251–1259. [CrossRef]

47. Lanfear, R.; Ho, S.Y.W.; Davies, T.J.; Moles, A.T.; Aarssen, L.; Swenson, N.G.; Warman, L.; Zanne, A.E.; Allen, A.P. Taller plants have lower rates of molecular evolution. *Nat. Commun.* **2013**, *4*, 836. [CrossRef]

48. Mahoney, D.J.; Jordan, D.L.; Hare, A.T.; Leon, R.G.; Roma-Burgos, N.; Vann, M.C.; Jennings, K.M.; Everman, W.J.; Cahoon, C.W. Palmer amaranth (*Amaranthus palmeri*) growth and seed production when in competition with peanut and other crops in North Carolina. *Agronomy* **2021**, *11*, 1734. [CrossRef]

49. Norsworthy, J.K.; Griffith, G.M.; Scott, R.C.; Smith, K.L.; Oliver, L.R. Confirmation and control of glyphosate-resistant Palmer amaranth (*Amaranthus palmeri*) in Arkansas. *Weed Technol.* **2008**, *22*, 108–113. [CrossRef]

50. Sosnoskie, L.M.; Webster, T.M.; Kichler, J.M.; MacRae, A.W.; Grey, T.L.; Culpepper, A.S. Pollen-Mediated Dispersal of Glyphosate-Resistance in Palmer Amaranth under Field Conditions. *Weed Sci.* **2012**, *60*, 366–373. [CrossRef]

51. Haubrock, P.J.; Cuthbert, R.N.; Haase, P. Long-term trends and drivers of biological invasion in Central European streams. *Sci. Total Environ.* **2023**, *876*, 162817. [CrossRef]

52. Liang, Y.; Li, J.; Li, J.; Valimaki, S.K. Impact of urbanization on plant diversity: A case study in built-up areas of Beijing. *For. Stud. China* **2008**, *10*, 179–188. [CrossRef]

53. Malkinson, D.; Kopel, D.; Wittenberg, L. From rural-urban gradients to patch–matrix frameworks: Plant diversity patterns in urban landscapes. *Landsc. Urban. Plan.* **2018**, *169*, 260–268. [CrossRef]

54. Mayer, K.; Haeuser, E.; Dawson, W.; Essl, F.; Kreft, H.; Pergl, J.; Pysek, P.; Weigelt, P.; Winter, M.; Lenzner, B.; et al. Naturalization of ornamental plant species in public green spaces and private gardens. *Biol. Invasions* **2017**, *19*, 3613–3627. [CrossRef]

55. Kuang, W.H. 70 years of urban expansion across China: Trajectory, pattern, and national policies. *Sci. Bull.* **2020**, *65*, 1970–1974. [CrossRef] [PubMed]

56. Irl, S.D.H.; Schweiger, A.H.; Steinbauer, M.J.; Ah-Peng, C.; Arevalo, J.R.; Beierkuhnlein, C.; Chiarucci, A.; Daehler, C.C.; Fernandez-Palacios, J.M.; Flores, O.; et al. Human impact, climate and dispersal strategies determine plant invasion on islands. *J. Biogeogr.* **2021**, *48*, 1889–1903. [CrossRef]

57. Fonseca, É.; Both, C.; Cechin, S.Z. Introduction pathways and socio-economic variables drive the distribution of alien amphibians and reptiles in a megadiverse country. *Divers. Distrib.* **2019**, *25*, 1130–1141. [CrossRef]

58. Ledda, A.; Yanniccari, M.; Franco, M.C.; Sobrero, M.T. Thermal time and extreme weather events determine the emergence of *Amaranthus palmeri*. *Adv. Weed Sci.* **2022**, *40*, e020220104. [CrossRef]

59.   Turner, N.C.; Molyneux, N.; Yang, S.; Xiong, Y.-C.; Siddique, K.H. Climate change in south-west Australia and north-west China: Challenges and opportunities for crop production. *Crop. Pasture Sci.* **2011**, *62*, 445–456. [CrossRef]

60.   Cao, J.J.; Wang, R.; Liu, W.X.; Wan, F.H.; Guo, J.Y. Invasion risk assessment of *Amaranthus palmeri* at different latitudinal regions in China based on seed germination rate. *J. Plant Prot.* **2022**, *48*, 8–15. [CrossRef]

61.   Wright, S.R.; Coble, H.D.; Raper, C.D.; Rufty, T.W. Comparative responses of soybean (*Glycine max*), sicklepod (*Senna obtusifolia*), and Palmer amaranth (*Amaranthus palmeri*) to root zone and aerial temperatures. *Weed Sci.* **1999**, *47*, 167–174. [CrossRef]

62.   Guo, P.; Al-Khatib, K. Temperature effects on germination and growth of redroot pigweed (*Amaranthus retroflexus*), Palmer amaranth (*A. palmeri*), and common waterhemp (*A. rudis*). *Weed Sci.* **2003**, *51*, 869–875. [CrossRef]

63.   Chahal, P.S.; Irmak, S.; Jugulam, M.; Jhala, A.J. Evaluating effect of degree of water stress on growth and fecundity of Palmer amaranth (*Amaranthus palmeri*) using soil moisture sensors. *Weed Sci.* **2018**, *66*, 738–745. [CrossRef]

64.   Sarangi, D.; Irmak, S.; Lindquist, J.L.; Knezevic, S.Z.; Jhala, A.J. Effect of water stress on the growth and fecundity of common waterhemp (*Amaranthus rudis*). *Weed Sci.* **2016**, *64*, 42–52. [CrossRef]

65.   Robinson, T.B.; Martin, N.; Loureiro, T.G.; Matikinca, P.; Robertson, M.P. Double trouble: The implications of climate change for biological invasions. *NeoBiota* **2020**, *62*, 463–487. [CrossRef]

66.   Kueffer, C. Plant invasions in the Anthropocene. *Science* **2017**, *358*, 724–725. [CrossRef] [PubMed]

67.   Bravo, W.; Leon, R.G.; Ferrell, J.A.; Mulvaney, M.J.; Wood, C.W. Differentiation of life-history traits among Palmer amaranth populations (*Amaranthus palmeri*) and its relation to cropping systems and glyphosate sensitivity. *Weed Sci.* **2017**, *65*, 339–349. [CrossRef]

68.   Cahoon, C.W.; York, A.C.; Jordan, D.L.; Everman, W.J.; Seagroves, R.W.; Culpepper, A.S.; Eure, P.M. Palmer amaranth (*Amaranthus palmeri*) management in dicamba-resistant cotton. *Weed Technol.* **2015**, *29*, 758–770. [CrossRef]

69.   Rockwell-Postel, M.; Laginhas, B.B.; Bradley, B.A. Supporting proactive management in the context of climate change: Prioritizing range-shifting invasive plants based on impact. *Biol. Invasions* **2020**, *22*, 2371–2383. [CrossRef]

70.   Tu, W.; Xiong, Q.; Qiu, X.; Zhang, Y. Dynamics of invasive alien plant species in China under climate change scenarios. *Ecol. Indic.* **2021**, *129*, 107919. [CrossRef]

71.   Sosnoskie, L.; Webster, T.; Grey, T.; Culpepper, A. Severed stems of *Amaranthus palmeri* are capable of regrowth and seed production in *Gossypium hirsutum*. *Ann. Appl. Biol.* **2014**, *165*, 147–154. [CrossRef]

72.   Bulletin, E. *Amaranthus palmeri* S. Watson. *Bull. OEPP* **2020**, *50*, 535–542.

73.   Anibaba, Q.A.; Dyderski, M.K.; Jagodziński, A.M. Predicted range shifts of invasive giant hogweed (*Heracleum mantegazzianum*) in Europe. *Sci. Total Environ.* **2022**, *825*, 154053. [CrossRef] [PubMed]

74.   Mosena, A.; Steinlein, T.; Beyschlag, W. Reconstructing the historical spread of non-native plants in the North American West from herbarium specimens. *Flora* **2018**, *242*, 45–52. [CrossRef]

75.   Chauvel, B.; Dessaint, F.; Cardinal-Legrand, C.; Bretagnolle, F. The historical spread of *Ambrosia artemisiifolia* L. in France from herbarium records. *J. Biogeogr.* **2006**, *33*, 665–673. [CrossRef]

76.   Rathore, M.K.; Sharma, L.K. Efficacy of species distribution models (SDMs) for ecological realms to ascertain biological conservation and practices. *Biodivers. Conserv.* **2023**, *32*, 3053–3087. [CrossRef]